Research Article

Mesoporous Co₃O₄ as a New Catalyst for Allylic Oxidation of Cyclohexene

H. Azzi[1,2*], I. Rekkab-Hammoumraoui[1], L. Chérif-Aouali[1], A. Choukchou-Braham[1]

[1]*Laboratoire de Catalyse et Synthèse en Chimie Organique, Université de Tlemcen, BP 119, Algeria*
[2]*Centre Universitaire de Ain Témouchent, Institut des Sciences et de la Technologie, BP 284, 46000 Ain Témouchent, Algeria*

Abstract

Mesoporous cobalt oxide was investigated for the liquid phase oxidation of cyclohexene using tertiobutylhydroperoxide (TBHP) as an oxidant. The results were compared with several series of supported cobalt catalysts to study the influence of the cobalt loading and solvents on the overall conversion and selectivity. Mesoporous cobalt was synthesized through the nanocasting route using siliceous SBA-15 mesoporous material as a hard template and cobalt nitrate as the cobalt oxide precursor. Supported cobalt oxide catalysts (Co/M_xO_y) were synthesized by the impregnation method using two loadings (1 and 5 wt.%) and Al_2O_3, TiO_2, and ZrO_2 as supports. Samples were characterised by means: elemental analysis, X-ray powder Diffraction (XRD), BET (surface area), UV-Vis DR Spectroscopy, and Transmission Electron Microscopy (TEM). The results obtained showed that the cobalt oxide retains the mesoporous structure of SBA-15, and in all Co/M_xO_y, crystalline Co_3O_4, and CoO phases are observed. The mesoporous cobalt oxide is more active than the supported cobalt catalysts in the allylic oxidation of cyclohexene, with a conversion of 78 % of cyclohexene and 43.3 % selectivity toward 2-cyclohexene-1-ol. The highest activity of mesoporous cobalt oxide could be ascribed to its largest surface area. Furthermore, Co_3O_4 has both Lewis and Brönsted acidic sites whereas Co/M_xO_y has only Lewis acidic sites, which could also explain its superior catalytic activity. Moreover, mesoporous cobalt oxide was more stable than supported cobalt catalysts. Therefore, this catalyst is promising for allylic oxidation of alkenes. Copyright © 2018 BCREC Group. All rights reserved

Keywords: Mesoporous Co_3O_4; Supported Cobalt; Cyclohexene; Allylic Oxidation

1. Introduction

In the petroleum industry a large amounts of alkane and alkene are produced as by-products which can be oxidized to oxygenated derivatives and converted into value-added products, such as: alcohols, ketones, aldehydes, and carboxylic acids [1].

During the allylic oxidation process, the reaction occurs on the C–H key in allyl of alkene to produce an alcohol and ketone and the C=C bond is retained [2,3]. When the reaction take place at C=C key, peroxide is generates. The oxidation of cylohexene has been the research topic of a large number of investigations because of the importance of the obtained prod-

* Corresponding Author.
  E-mail: hajer.azzi@cuniv-aintemouchent.dz (H. Azzi)

ucts, like the cyclohexene oxide, 2-cyclohexene-1-one [4,5] and 2-cyclohexene-1-ol [5-8]. The 2-cyclohexen-1-ol (enol) can be converted to phenol without co-products. The 2-cyclohexen-1-one (enone) is extensively utilized in the synthesis of drugs, pesticides and adipic acid which is utilized in nylon-6 manufacture. The synthesis of fine chemicals uses cyclohexene oxide as a key intermediate owing to its high reactivity which is ascribed to the opening of the highly strained three-membered ring [9,10].

Although the homogeneous catalysts have a high activity in the oxidation reactions, however they have significant disadvantages in the recovery of the catalyst and the isolation of the product. In contrast, heterogeneous catalysts systems exhibit high activity, stability, and reusability. Various cobalt-substituted mesoporous materials have been investigated as catalysts for selective liquid phase oxidation [5,11-14].

Zhen *et al.* [15] reported that cobalt oxide in the form of nanocrystalline particles is a crucial factor for attaining high activity for combustion of VOCs, CO oxidation, and NO_2 decomposition [15]. Hence, the synthesis of nanostructured cobalt oxides especially with ordered mesoporous structure has been investigated [15,16]. Mesoporous Co_3O_4 has exhibited a higher catalytic activity in the combustion of VOCs than that obtained by a conventional Co_3O_4. To the best of our knowledge this is the first report investigating mesoporous Co_3O_4 as a catalyst for selective liquid phase oxidation.

In this paper, mesoporous Co_3O_4 was prepared via the nanocasting route using mesoporous SBA-15 silica as a mold and cobalt nitrate as a precursor through a solid-liquid route [17]. Mesoporous cobalt oxide was investigated for the liquid phase oxidation of cyclohexene using tertiobutylhydroperoxide (TBHP) as an oxidant. The results were compared with several series of supported cobalt catalysts to study the influence of the cobalt loading and solvents on the overall conversion and selectivity.

2. Materials and Method

2.1 Catalysts Preparation

2.1.1 Mesoporous cobalt oxide (Co_3O_4)

Synthesis of the mesoporous silica SBA-15 was conducted in a way similar to that used by Zhao *et al.* [18]. The mesoporous cobalt oxide was obtained using the method given below, i.e. 1 mmole of the precursor $Co(NO_3)_x.yH_2O$ was combined with 0.15 g of SBA-15 and the mix was then crushed for a short moment in an agate mortar and pestle. Next, the admixture was placed in a melting pot that was put in a muffle furnace, where the temperature was raised from ambient temperature to 400 °C, at a rate of 1 °C/min; it was then maintained at the final value for the period of 5 hours. After that, the sample was cooled down back to ambient temperature. A 10 %wt. HF aqueous solution was used to remove the silica template. Centrifugation was used to recuperate the mesoporous cobalt oxide which was then washed with distilled water trees times.

2.1.2 Supported Co/M_xO_y

The supports, such as: Al_2O_3 (Oxid C Degussa), TiO_2 (Titandioxid Degussa), and ZrO_2 (Aldrich), are all available on the market; they are in the form of a nanopowder (nanoparticles in the range from 10 to 50 nm). A preliminary treatment is required before the metal precursors are impregnated.

The chosen supports were mixed with water (an amount of 200 mL of H_2O with 100 g of support) in order to obtain a paste. This mixture was left to dry overnight at the temperature of 120 °C, and was then sifted in order to hold back only the particles with a diameter that is between 1 and 2.5 Å. After that, the support was calcined at the temperature of 400 °C under oxidative flow (20 % O_2, 80 % Ar, 60 mL/min) for a period of 4 hours. These oxides were next impregnated with an aqueous solution of $Co(NO_3)_2.6 H_2O$ (Fluka) in order to get 1 and 5 %wt. of cobalt catalyst. First, the solvent was evaporated, next the solids were dried at the temperature of 120 °C overnight, and then they were calcined at 400 °C.

2.2 Catalysts Characterization

Instrumental analyses have been employed to investigate the physicochemical characteristics of the prepared catalysts. The metal content was checked by Inductively Coupled Plasma Atomic Emission Spectroscopy (ICP-AES) using an OPTIMA 2000 DV spectrometer. The surface areas and pore sizes were measured by nitrogen adsorption at 77 K on a Micrometrics Tristar 3000 apparatus after heat pre-treatment under vacuum for 6 hours at 250 °C. The acidity contents were determined by Fourier Transform Infra Red (FTIR) analysis of chemisorbed pyridine using a Nicolet Magna IR spectrometer. Details on the experimental procedure have been described in previous works [4,19].

Wide angle powder X-ray Diffraction (XRD) patterns were collected on a Bruker D5005 dif-

fractometer, using a Cu-Kα radiation (λ = 1.54 Å). For small-angle analysis, the XRD patterns were collected on a Bruker AXS D5005 X-ray source; the signal was recorded for 2θ comprised between 0.7 and 5 °. DRS spectra of the samples studied were recorded in the wavelength range 200-800 nm at room temperature, using a UV-Vis spectrophotometer (Perkin Elmer) with KBr as the reference. The size and dispersion of the Co particles were observed using Transmission Electron Microscopy (TEM) in conjunction with energy dispersive X-ray Spectroscopy (EDXS). Micrographs are obtained on a JEOL 2100 instrument (operated at 2200 KV with a LaB6 source and equipped with a Gatan Ultra Scan camera).

2.3 Catalytic Reactions

Tertiobutylhydroperoxide TBHP (Aldrich, 70 wt.% in H_2O) was used as an oxidant for the catalytic oxidation of cyclohexene in a two-neck glass round bottom flask fitted with a magnetic stirrer and a reflux condenser. Firstly, the solvent and TBHP were mixed and well agitated to achieve a phase transfer from water to organic phase.

Normally, 20 mL of solvent and 5.5 mL of oxidant (TBHP) were blended into a closed erlenmeyer flask and magnetically agitated for a period of 24 hours. Next, the organic phase contained was isolated from the aqueous phase. The concentration of the TBHP that remained in the aqueous phase was determined by iodometric titration in order to control the phase transfer. The quantity of TBHP that remained in the aqueous phase was less than 10 % of the initial amount. After that, the TBHP-solvent mixture, 3 mL of cyclohexene, and 0.1 g of catalyst were admixed in the magnetic stirrer-glass reactor, at 343 K and stirred for a period of 6 hours.

Identification of the reaction products was done by comparing them with authentic ones. The course of the reactions was monitored by gas chromatography (GC), using a YL6500 GC system equipped with an Agilent HP-FFAP capillary column and a flame ionization detector (FID). The remaining TBHP was decomposed before the GC analysis by incorporating an excess of triphenylphosphine (Aldrich). Moreover, an iodometric titration was carried out at the end of the reaction (after 6 h) by analysing the organic phase, in order to control the remaining TBHP. The catalytic performances were reported in terms of cyclohexene conversion, selectivity towards products and turnover frequency. They are calculated following the Equations (1-2).

$$Conversion \; (\%) = \frac{[C_6H_{10}]_0 - [C_6H_{10}]_t}{[C_6H_{10}]_0} x100 \qquad (1)$$

$$Selectivity(\%) = \frac{Moles\,of\,individual\,product}{Moles\,of\,total\,product} x100 \qquad (2)$$

3. Results and Discussion

3.1 Catalysts Characterization

3.1.1 N_2 Adsorption-desorption isotherms

N_2 adsorption-desorption isotherms and pore size distribution of Co_3O_4 are presented in Figure 1. The textural properties of Co_3O_4 and supported cobalt oxide catalysts are listed in Table 1. Figure 1 shows that Co_3O_4 has a jump at P/P_0= 0.8-1.0 which is typical for mesoporous solids indicating that the mesoporous structure is retained in the nanocasting process via a solid-liquid route [20,21]. As shown in Table 1, mesoporous Co_3O_4 exhibits a larger surface area than those of supported catalysts.

It is important to note that the surface area of mesoporous Co_3O_4 synthesized in this work by the nanocasting pathway via a solid-liquid route is much higher than those of mesoporous Co_3O_4 synthesized by the nanocasting pathway via the solvent evaporation method [22,23]. The lower surface area of mesoporous Co_3O_4 as compared to SBA15 silica can partly be ascribed to the difference between the densities of the two materials, as reported for mesoporous MgO synthesized by the nanocasting pathway [24]. Bulk Co_3O_4 has a density of 6.11 g/cm³ while that of amorphous SiO_2 is 2.2 g.cm⁻³. It is reasonable to suppose analogous differences in the densities for the pore
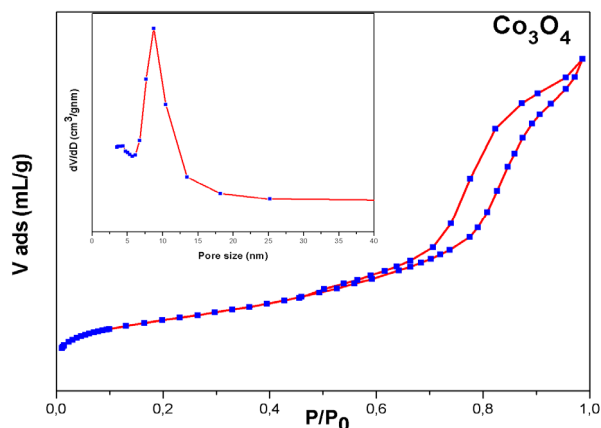

Figure 1. N_2 adsorption-desorption isotherms and BJH pore size distribution of Co_3O_4

walls of the two mesoporous materials; therefore, the surface areas of mesoporous Co_3O_4 and SBA-15 silica are closer to each other when normalized with respect to the density. The lower surface area of mesoporous Co_3O_4 is also attributed to the partial loss of structural order, which is in agreement with the XRD results.

3.1.2 Acid properties of catalysts

Pyridine adsorption is still one of the most frequently used methods for evaluating the acidity of solids. The infrared spectrum in the region between 1400 and 1700 cm^{-1} has been determined for pyridine adsorbed on acidic solids. FTIR spectra of pyridine adsorbed on 5 wt% Co/Al_2O_3, 5 wt% Co/ZrO_2, and 5 wt% Co/TiO_2 (not shown) showed only the 1455 cm^{-1} band which is typical of Lewis sites. No characteristic bands of pyridine adsorption on Brönsted acid sites were seen (formation of the pyridinium ion leading to two adsorption bands at 1545 cm^{-1} and 1637 cm^{-1}) [25,26].

The FT-IR spectrum of mesoporous Co_3O_4 showed both Lewis acid site bands and Brönsted acid site bands at 1446 and 1554 cm^{-1}, respectively. The data summarized in Table 1 indicate that mesoporous Co_3O_4 possesses significant Brönsted and Lewis acidity. The Co/Al_2O_3 sample was found to be more acidic (150 μmol.g^{-1} at 150 °C) than Co/ZrO_2 (52 μmol.g^{-1} at 150 °C) and Co/TiO_2 (6 μmol.g^{-1} at 150 °C). The cobalt loading measured by ICP-AES is 1 or 5 wt% in all supported materials.

3.1.3 XRD characterizations

The XRD patterns of the samples are presented in Figure 2. The low-angle XRD pattern of Co_3O_4 (Figure 2a) shows one diffraction corresponding to (100) reflection which can be related with the hexagonal symmetry characteristic of mesoporous SBA-15 [27] showing that the mesoporous structure is retained in the nanocasting process via a solid-liquid route. It
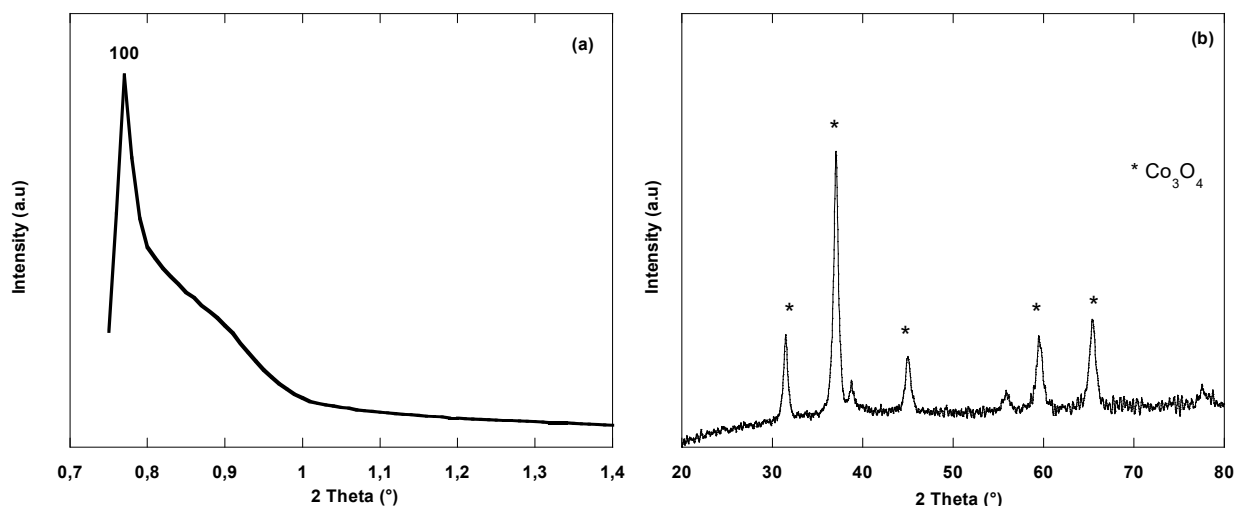

Figure 2. XRD of mesoporous Co_3O_4: Low angle (a) and Wide angle (b)

Table 1. Textural properties of supports, Lewis, and Brönsted acidity and metal content of catalyst

Catalyst	ICP-AES (wt.%)	Lewis acidity (μmol.g^{-1})	Brönsted acidity (μmol.g^{-1})	Textural properties of supports		
				Surface area (m^2.g^{-1})	Pore size (nm)	Pore volume (cm^3.g^{-1})
Co_3O_4	-	193	241	164	9	0.34
Co/Al_2O_3	1.07	-	-	-	-	-
	5.08	150	-	95	31	0.72
Co/ZrO_2	0.92	-	-	-	-	-
	5.07	52	-	35	30	0.26
Co/TiO_2	0.87	-	-	-	-	-
	4.76	6	-	43	26	0.27

is worth noting a certain degree of broadening of the reflections which indicate some loss in structural order.

Figure 2b shows the wide-angles XRD patterns; on the Co_3O_4 pattern the diffraction peaks at 2θ = 19.08°, 31.38°, 36.88°, 44.88°, 59.38°, and 65.28° are ascribed to Co_3O_4 in the cubic phase with Fd3m space group (JCPDS no. 42-1467) [28]. On all Co/ M_xO_y patterns (Figure 3), crystalline Co_3O_4 and CoO phases are observed and metallic Co is not detected. In addition, the diffraction peaks at 2θ = 34.5° and 42.4° could be attributed to CoO in the cubic form (JCPDS no. 71-1178) [29,30]. For 5 % Co/Al_2O_3, the diffraction peaks at 2θ = 37°, 45°, and 66° are attributed to g Al_2O3 [31] and for 5 wt% Co/ZrO_2, the diffraction peaks at 2θ = 28.17°, and 31.47° are ascribed to the presence of ZrO_2 in the monoclinic phase (JCPDS no. 37-1484), and the peak at 30.12° indicates the presence of zirconia in the face centered cubic form (JCPDS no. 49-1642). On Co/TiO_2 pattern, the simultaneous presence of rutile (JCPDS no. 21-1276) and anatase (JCPDS no. 21-1272) phases are detected indicating that TiO_2 is constituted of a mixture of titanium oxide in the quadratic and centered quadratic phases.

3.1.4 DR-UV-Vis analysis

Diffuse-reflectance UV-Vis spectroscopy is a sensitive tool that is frequently used to detect the environment of cobalt. Mesoporous cobalt oxide spectrum is characterized by the presence of six bands (Figure 4). The bands centered at about 410 nm and 720 nm are assigned to O^{2-}–Co^{2+} and O^{2-}–Co^{3+} charge transfer processes, respectively [32-34], indicating the formation of Co_3O_4 which in agreement with the XRD results. The peak intensity at 400 nm on

mesoporous Co_3O_4 was higher than that at 700 nm, which indicate the importance of Co^{2+} species on this catalyst. The bands at 320 nm, 520 nm, and 620 nm are ascribed to the presence of Co^{2+} in the tetrahedral coordination [35,36]. The absorption band at 248 nm can be assigned to NO_3^- ions present inside the pores [37].

The UV-vis-spectra of the catalysts supported cobalt Co/M_xO_y (Figure 5) exhibit strong band at ~240 nm originating from the oxygen-to-metal charge transfer transitions [38]. The spectrums show a triplet at 320, 500, and 600 nm, characteristic of the presence of Co^{2+} ions in tetrahedral coordination. Two others bands at 400 and 670 nm could be assigned to octahedral Co^{3+} ion similarly to that in Co_3O_4 [34,39-32].

3.1.5 TEM characterizations

Figures 6 and 7 present TEM images of the cobalt based catalysts. Figure 6 shows, in accordance with the XRD and N_2 adsorption-desorption results, the mesoscopic order of Co_3O_4, indicating that cobalt oxide retains the SBA-15 mesostructure. For 5 % Co/Al_2O_3 (Figure 7a) and 5 % Co/ZrO_2 (Figure 7b) of TEM analysis reveals an intensive agglomeration of cobalt particles on these samples and, then, a true reliable distribution cannot be given. The average size of these agglomerations is between 8 nm and 10 nm.

4. Catalytic Activity

4.1 Oxidation of Cyclohexene

The cyclohexene oxidation with tert-butyl hydroperoxide (TBHP) as oxidant was used to assess the catalytic activity of the as-prepared
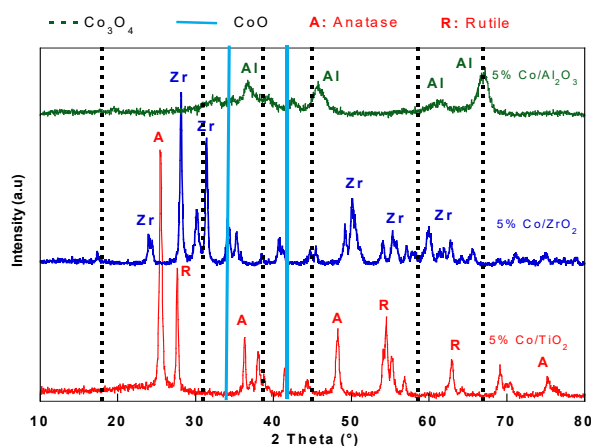

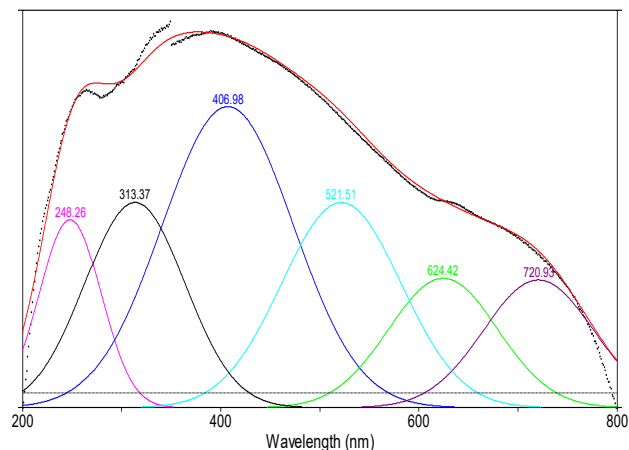**Figure 3.** X-ray diffraction (XRD) patterns of samples

Figure 4. DR-UV-vis spectra of Co_3O_4

catalysts. It should be noted that Al_2O_3, ZrO_2, and TiO_2 supports are inactive in this reaction.

The cyclohexene oxidation can give six products: cyclohexene epoxide (Epo); 2-cyclohexene-1-ol (enol); 2-cyclohexene-1-one (enone); cyclohexanol (ol); cyclohexanone (one); and cyclohexene-1,2-diol. A possible mechanism of cyclohexene oxidation has been proposed; it involves two main paths. The first one is a direct epoxidation, in the presence of redox catalysts, leading to the epoxide, which may be transformed into a diol in the presence of water and an acidic medium. The second one is an allylic oxidation which, in the presence of Lewis acid sites and redox centers, may give 2-cyclohexene-1-ol (enol), 2-cyclohexene-1-one (enone), cyclohexanone, and cyclohexanol [43] as illustrated in the following catalytic scheme (Figure 8).

Our catalysts drive the reaction selectivity towards the allylic oxidation due to their strong acidity [4,25,44]. The orientation of the reaction towards the formation of 2-cyclohexene-1-ol as majority product indicates the preferential attack of the activated C–H bond over the C=C bond. It is important to mention that, the 2-cyclohexene-1-one, was only detected in presence of Co_3O_4 mesoporous oxide (Table 2).

From the results shown in Table 2 we note: The mesoporous cobalt oxide has a better activity with 78 % of conversion compared to Co/M_xO_y catalysts. Co_3O_4 exhibits a larger surface area than those of supported catalysts (Table 1) which could explain the highest catalytic activity of this catalyst. Additionally, Co_3O_4 has both Lewis and Brönsted acidic sites
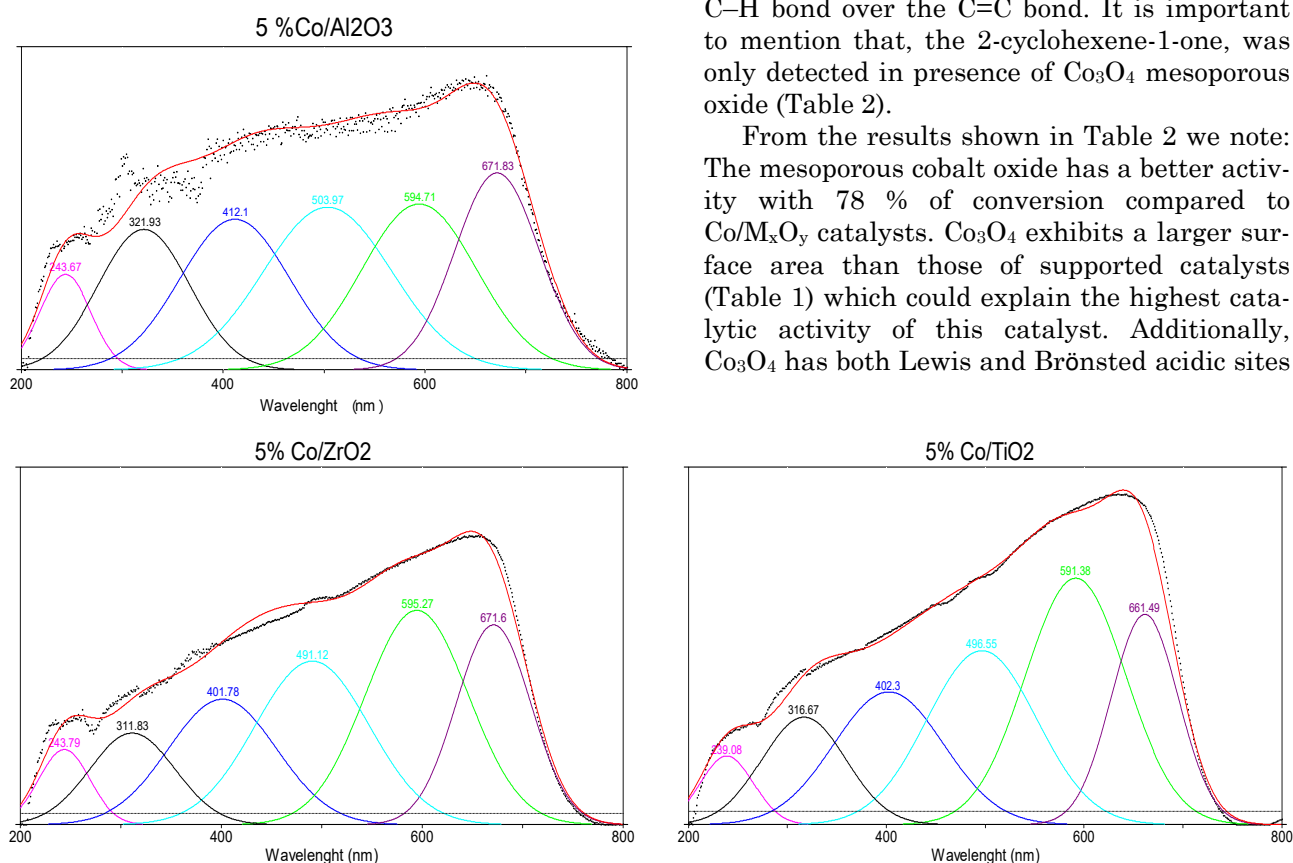

Figure 5. DR-UV-vis spectra of supported catalysts: (a) Co/Al_2O_3; (b) Co/ZrO_2; (c) Co/TiO_2

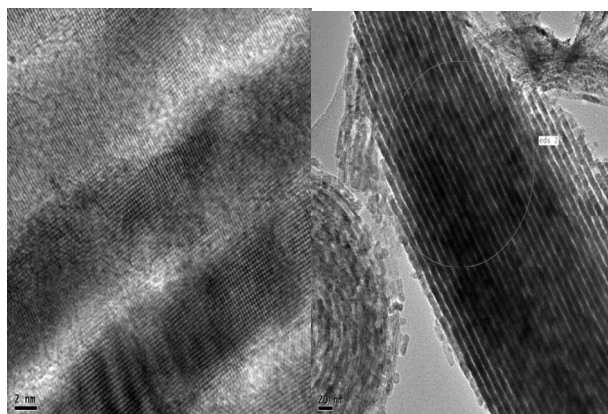**Figure 6.** TEM images of mesoporous Co_3O_4

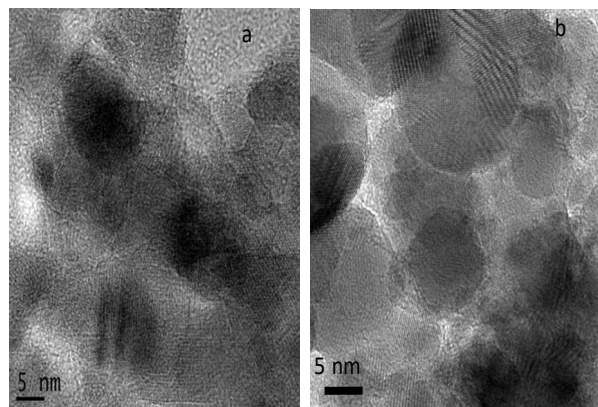**Figure 7.** TEM photos of catalysts: 5 % Co/ Al_2O_3 (a), 5% Co/ZrO_2 (b)

whereas Co/M_xO_y have only Lewis acidic sites (Table 1), which could also explain its superior catalytic activity, so it can be suggested that the presence of Brönsted acidic sites improves the catalytic activity in the cyclohexene oxidation.

The catalytic behavior of Co/M_xO_y towards cyclohexene oxidation was found to enhance with cobalt loading. When the Co content increased (from 1 to 5 %), the 2-cyclohexen-1-ol selectivity decreased slightly with concomitant formation of other oxidized products with com-

parable amounts: cyclohexene-1,2-diol (1.7 %), cyclohexene epoxide (2.4 %), cyclohexanol (3.7 %) and cyclohexanone (5.3 %).

These results could be explained in terms of the Lewis acidity of the catalysts. It is well established in the literature that the acidity jointly with the redox properties of the metal determine the selectivity of the catalyst towards oxidation products [45]. Moreover, the contribution of Lewis acid sites in the oxidation of cyclohexene has many times been stressed in the literature [45-47].
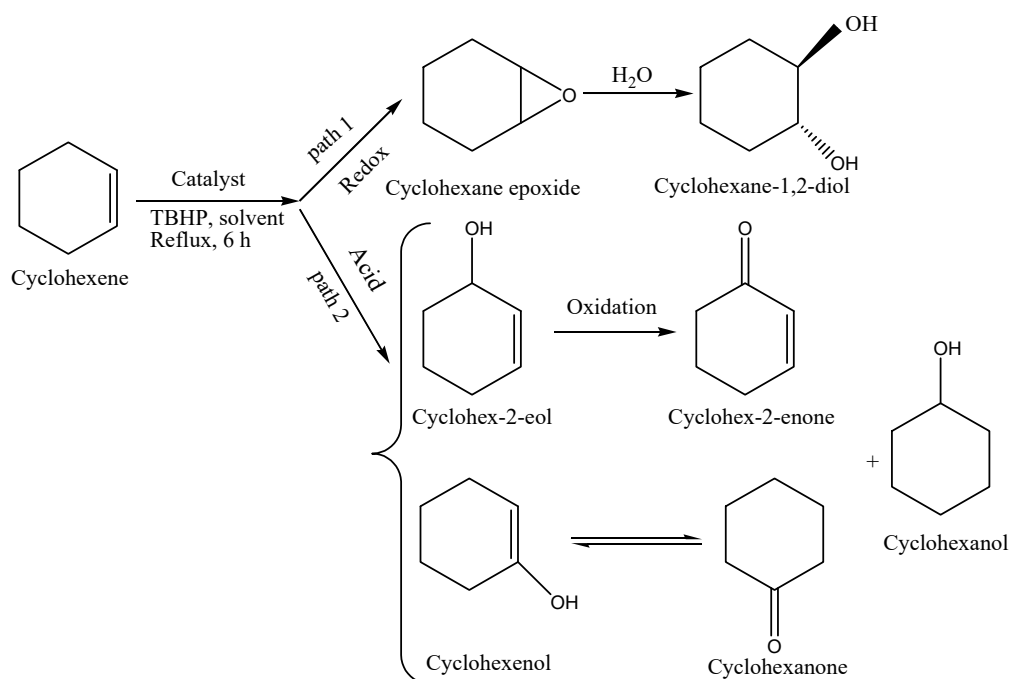

Figure 8. Different pathways for cyclohexene oxidation reaction

Table 2. Oxidation of cyclohexene with different catalysts

Catalyst	wt. (%)	Conv. (%)	Selectivity (%)						TBHP consumption (%)
Co₃O₄	/	45	6	50	32	0	12	0	75
		78[a]	0[a]	43[a]	41[a]	0[a]	16[a]	0[a]	81
Co/Al₂O₃	5.08	13	2	87	0	4	5	2	16
		44[a]	4[a]	48[a]	0[a]	27[a]	12[a]	9[a]	53
	1.07	5	2	96	0	0	2	0	14
Co/ZrO₂	5.07	7	3	96	0	1	0	0	16
	0.92	3	0	98	0	0	2	0	16
Co/TiO₂	4.76	11	0	95	0	2	1	2	14
	0.87	5	0	97	0	0	1	2	16

TBHP = 39.73 mmol (5.5 mL); Solvent:heptane (20 mL); C_6H_{10} = 29 mmol (3 mL); Catalyst = 0.1 g T = 70 °C.
[a]: solvent: acetic acid

The results reveal (Table 1) that all Co/M_xO_y systems seem to have the following relative order of Lewis acidity: $Co/Al_2O_3 > Co/ZrO_2 > Co/TiO_2$. This Lewis order of acidity is in agreement with the catalyic activity of our samples and also with other results previously reported in the literature [48]. On other hand, TBHP as oxidant promotes the allylic oxidation pathway and minimizes the epoxidation, particularly under the highly acidic properties of catalysts [49].

It is well known that the nature of solvents used has a major impact on the reaction kinetics and product selectivity in the oxidation of cyclohexene. The oxidation reaction was carried out in polar protic solvent (acetic acid) in presence of Co_3O_4 and 5 %Co/Al_2O_3 the most acidic catalyst among the 5 %Co/M_xO_y catalysts (Table 2). It has been found that 2-cyclohexene-1-ol was formed as the major product with high conversion (78 %) and selectivity (43.3 %) over mesoporous Co_3O_4. Obviously, the catalyst surface prefers to adsorb the more polar molecules, such as ketone and alcohol molecules, which are able to block the active sites of the catalyst. Then, the polar solvent could wash out the other products from the surface and consequently the oxidant and cyclohexene would have more chance to reach the active sites [50,51]. Moreover, the acetic acid acts as an oxidizing agent (formation of the peracetic acid complex) [19].

4.2 Reusability of the Catalyst

The catalytic stability of mesoporous Co_3O_4 and 5 % Co/Al_2O_3 in cyclohexene oxidation is studied (Table 3). The catalyst was reused for a new run after it was separated from the reaction mixture through filtration, washed with water and dried at 100 °C.
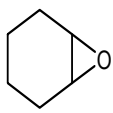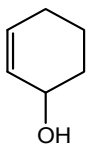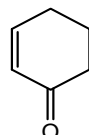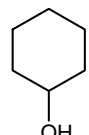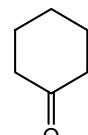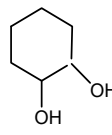
For mesoporous Co_3O_4, the activity of the refreshed catalyst after the first cycle remains the same as that of fresh catalyst and decreases of 21.8 % and 34.6 % for the 3rd and 4rd runs, respectively. It is also noted that the selectivity changes slightly, the appearance of the diol after the first cycle is probably due to the presence of the water framework, adsorbed during the course of the reaction. In contrast, 5 %Co/Al_2O_3 loses its activity under recycling. The deactivation of the catalyst is probably related to frequent inhibition processes found in oxidation reactions such, as the adsorption of oxygenated species on the catalyst surfaces [3].

Leaching of the metal into solution was checked by AAS analyses of the supernatant solution (Table 3). We found that a negligible amount of cobalt was leached into solution when mesoporous Co_3O_4 was used as catalyst, so it is not the likely reason for the catalyst deactivation. In contrast, a higher metal leaching (3.61 %.) was observed for Co/Al_2O_3.

In order to confirm that mesoporous Co_3O_4 acts truly as a heterogeneous catalyst, it was separated by filtration from the reaction mixture and the reaction was allowed to continue on the remaining filtrate solution for another 2 h under the same reaction conditions; no further conversion of cyclohexene was observed, showing that the oxidation of cyclohexene over mesoporous Co_3O_4 is purely heterogeneous.

In order to investigate the causes for the decrease in the activity during the recycling experiment, the spent Co_3O_4 catalysts were characterized by XRD and N_2 physisorption.

Table 3. Recycling results of the catalysts

Catalyst	wt. (%)	Conv. (%)	Selectivity (%)						wt% Co[a]
			epoxide	OH	=O	OH	=O	OH/OH diol	
Co_3O_4	1st	78	6	49	33	0	12	0	0.29
	2nd	78	2	44	25	0	31	8	0.35
	3rd	61	0	38	21	0	28	13	0.19
	4th	51	0	41	23	0	24	12	0.16
5% Co/Al_2O_3	1st	44	4	48	0	26	13	9	2.1
	2nd	37	0	46	0	26	16	15	3.61
	3rd	31	0	45	0	24	14	17	3.46
	4th	12	0	46	0	24	11	19	1.04

TBHP = 39.73 mmol (5.5 mL); Solvent: Acetic acid (20 mL); C_6H_{10} = 29 mmol (3 mL); Catalyst = 0.1 g T = 70
a: cobalt content (wt%) leached into solution

It can be seen from Figure 9 that the XRD patterns of fresh and spent catalysts are similar, indicating that the ordered structure of Co_3O_4 is not affected during the recycling experiment, showing that the catalytic system can be reused without loss of catalyst's structure.

In contrast, the textural properties of Co_3O_4 catalysts are affected during the recycling experiment (Table 4), the BET surface area and the pore volume decrease, which is attributed to clogging catalyst pores by carbonaceous species that makes them inaccessible for nitrogen adsorption. These carbonaceous species, formed inside the catalyst porosity through secondary reaction between the reaction products, block the pore access of the catalyst, leading to a deactivation during the reuse. The spent catalyst can be easily regenerated by calcination in air at 500 °C.

5. Conclusions

This study demonstrates that mesoporous Co_3O_4 is more active than supported cobalt oxide catalysts for allylic oxidation of cyclohexene with TBHP as an oxidant. The superior catalytic activity of mesoporous Co_3O_4 coul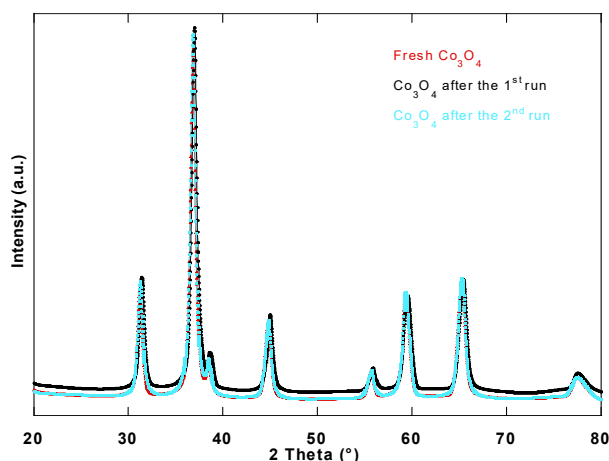d be explained by its larger surface area compared to those of supported materials (Co/M_xO_y). Indeed, a high surface area often leads to a greater activity due to an increased dispersion of active sites.

Additionally, Co_3O_4 has both Lewis and Brönsted acidic sites whereas Co/M_xO_y have only Lewis acidic sites, which could also explain its higher catalytic activity. Indeed, a high surface area often leads to a greater activity due to an increased dispersion of active sites. Moreover, mesoporous cobalt oxide is more stable than supported cobalt catalysts and it can be regarded as self-supported nanoscale catalysts; it does not need any support, as required by normal nanoparticle catalysts. Therefore, this catalyst is promising for allylic oxidation of alkenes.

Acknowledgment

References

[1] Gökçe, S., Saka, E.T., Bıyıklıoğlu; Z., Kantekin, H. (2013). Synthesis, Characterization of Metal-Free, Metallophthalocyanines and Catalytic Activity of Cobalt Phthalocyanine in Cyclohexene Oxidation. *Synthetic Metals*, 176: 108-115.

[2] Murphy, E.F., Mallat, T., Baiker, A. (2000). Allylic Oxofunctionalization of Cyclic Olefins with Homogeneous and Heterogeneous Catalysts. *Catalysis Today*, 57: 115-126.

[3] Silva, F.P., Jacinto, M.J., Landers, R., Rossi, L.M. (2011). Selective Allylic Oxidation of Cyclohexene by a Magnetically Recoverable Cobalt Oxide Catalyst. *Catalysis Letters*, 141: 432-437.

[4] Dali, A., Rekkab-Hammoumraoui, I., Choukchou-Braham, A., Bachir, R. (2015). Allylic Oxidation of Cyclohexene over Ruthenium-Doped Titanium-Pillared Clay, *RSC Advances*, 5: 29167-29178.

[5] Luque, R., Badamali, S.K., Clark, J.H., Fleming, M., Macquarrie, D.J. (2008). Controlling Selectivity in Catalysis: Selective Greener Oxidation of Cyclohexene under Microwave Conditions. *Applied Catalysis A: General*, 341: 154-159.

[6] Choi, B.G., Song, R., Nam, W., Jeong, B. (2005). Iron Porphyrins Anchored to a Thermosensitive Polymeric Core-Shell Nanosphere as a Thermotropic Catalyst. *Chemical Communications*, 0: 2960-2962.

Figure 9. XRD patterns of fresh and used catalysts

Table 4. Textural properties of fresh and used catalysts

Catalyst	Surface area ($m^2.g^{-1}$)	Pore size (nm)	Pore volume ($cm^3.g^{-1}$)
Fresh Co_3O_4	164	9	0.34
Co_3O_4 after the 1st run	144	8.3	0.22
Co_3O_4 after the 2nd run	50	5.6	0.15

[7]   Mukherjee, S., Samanta, S., Bhaumik, A., Ray, B.C. (2006). Mechanistic Study of Cyclohexene Oxidation and Its Use in Modification of Industrial Waste Organics. *Applied Catalysis B: Environmental*, 68: 12-20.

[8]   Serwicka, E.M., Połtowicz, J., Bahranowski, K., Olejniczak, Z., Jones, W. (2004). Cyclohexene Oxidation by Fe-, Co-, and Mn-Metalloporphyrins Supported on Aluminated Mesoporous silica. *Applied Catalysis A: General*, 275: 9-14.

[9]   Bhattacharjee, S., Anderson, J.A. (2006). Comparison of the Epoxidation of Cyclohexene, Dicyclopentadiene and 1,5-Cyclooctadiene over LDH Hosted Fe and Mn Sulfonato-Salen Complexes. *Journal of Molecular Catalysis A: Chemical*, 249: 103-110.

[10] Samantaray, S.K., Parida, K. (2005). Amine-Modified Titania–Silica Mixed Oxides: 1. Effect of Amine Concentration and Activation Temperature towards Epoxidation of Cyclohexene. *Catalysis Communications*, 6: 578-581.

[11] Anand, C., Srinivasu, P., Mane, G.P., Talapaneni, S.N., Benzigar, M.R., Vishnu Priya, S., Al-deyab, S.S., Sugi, Y., Vinu, A. (2013). Direct Synthesis and Characterization of Highly Ordered Cobalt Substituted KIT-5 with 3D Nanocages for Cyclohexene Epoxidation. *Microporous and Mesoporous Materials*, 167: 146-154.

[12] Habibi, D., Faraji, A.R., Arshadi, M., Heydari, S., Gil, A. (2013). Efficient Catalytic Systems Based on Cobalt for Oxidation of Ethylbenzene, Cyclohexene and Oximes in the Presence of N-hydroxyphthalimide. *Applied Catalysis A: General*, 466: 282-292.

[13] Mahdavi, V., Hasheminasab, H.R. (2015). Liquid-Phase Efficient Oxidation of Cyclohexane over Cobalt Promoted VPO Catalyst using Tert-Butylhydroperoxide. *Journal of the Taiwan Institute of Chemical Engineers*, 51: 53-62.

[14] Salavati-Niasari, M., Hassani-Kabutarkhani, M., Davar, F. (2006). Alumina-supported Mn(II), Co(II), Ni(II) and Cu(II) N,N-Bis(salicylidene)-2,2-dimethylpropane-1,3-diamine Complexes: Synthesis, Characterization and Catalytic Oxidation of Cyclohexene with Tert-Butylhydroperoxide and Hydrogen Peroxide. *Catalysis Communications*, 7: 955-962.

[15] Zhen, M., Zhou, B., Ren, Y. (2012). Crystalline Mesoporous Transition Metal Oxides: Hard-Templating Synthesis and Application in Environmental Catalysis. *Frontiers of Environmental Science & Engineering*, 7: 341-355.

[16] Gu, D., Jia, C.J., Weidenthaler, C., Bongard, H.J., Spliethoff, B., Schmidt, W., Schuth, F. (2015). Highly Ordered Mesoporous Cobalt-Containing Oxides: Structure, Catalytic Properties, and Active Sites in Oxidation of Carbon Monoxide. *Journal of the American Chemical Society,* 137: 11407-11418.

[17] Yue, W., Zhou, W. (2007) Synthesis of Porous Single Crystals of Metal Oxides via a Solid-Liquid Route. *Chemistry of Materials*, 19: 2359-2363.

[18] Zhao, D., Feng, J., Huo, Q., Melosh, N., Frederickson G.H., Chmelka, B.F., Stucky, G.D. (1998). Triblock Copolymer Syntheses of Mesoporous silica with Periodic 50 to 300 Angstrom Pores. *Science*, 279: 548-552.

[19] Rekkab-Hammoumraoui, I., Choukchou-Braham, A., Pirault-Roy, L., Kappenstein, C. (2011). Catalytic Oxidation of Cyclohexane to Cyclohexanone and Cyclohexanol by Tert-Butyl Hydroperoxide over Pt/Oxide Catalysts. *Bulletin of Materials Science*, 34: 1127-1135.

[20] Azzi, H., Bendahou, K., Cherif-Aouali, L., Hamidi, F., Siffert, S., Bengueddach, A., Aboukais, A. (2012). Total Oxidation of Toluene over Pd/Mesoporous Materials Catalysts. *Chemistry Today*, 30: 28-31.

[21] Bendahou, K., Cherif, L., Tidahy, H. L., Benaïssa, H., Aboukaïs, A. (2008). The Effect of the Use of Lanthanum-Doped Mesoporous SBA-15 on the Performance of Pt/SBA-15 and Pd/SBA-15 Catalysts for Total Oxidation of Toluene. *Applied Catalysis A: General*, 351: 82–87.

[22] Yu, R., Feng, J., Peter G.B. (2009). Tailoring the Pore Size/Wall Thickness of Mesoporous Transition Metal Oxides. *Microporous and Mesoporous Materials*, 121: 90–94 .

[23] Yunsheng, X., Hongxing, D., Haiyan, J., Lei, Z. (2010). Three-Dimensional Ordered Mesoporous Cobalt Oxides: Highly Active Catalysts for the Oxidation of Toluene and Methanol. *Catalysis Communications*, 11: 1171–1175.

[24] Jan, R., Gu̇nter, K., Michael, T. (2006). Synthesis of Mesoporous Magnesium Oxide by CMK-3 Carbon Structure Replication. *Chemistry of Materials*, 18: 4151- 4156

[25] Belaidi, N., Bedrane, S., Choukchou-Braham, A., Bachir, R. (2015). Novel Vanadium-Chromium-Bentonite Green Catalysts for Cyclohexene Epoxidation. *Applied Clay Science*, 107: 14-20

[26] Jankovic, L. (2003). Metal Cation-Exchanged Montmorillonite Catalyzed Protection of Aromatic Aldehydes with Ac_2O. *Journal of Catalysis*, 218: 227-33.

[27] Azzi, A., Cherif-Aouali, L., Siffert, S., Royer, S., Aissat, A., Cousin, R., Pronier, S., Bengueddach, A. (2014). The Effect of the Nature of Support on the Performance of Gold Supported Catalysts for Total Oxidation of Toluene. *Topics in Chemistry and Material Science*, 7: 84-91.

[28] Bao, A., Liew, K., Li, J. (2009). Fischer–Tropsch Synthesis on CaO-Promoted Co/Al$_2$O$_3$ Catalysts. *Journal of Molecular Catalysis A: Chemical*, 304: 47-51.

[29] Chen, H., Wang, B., Ma, H., Cui, X. (2008). Oxidation and Isomerization of Cyclohexane Catalyzed by SO$_4^{2-}$/Fe$_2$O$_3$-CoO under Mild Condition. *Journal of Hazardous Materials*, 150: 300-307.

[30] Shim, H.S., Shinde, V.R., Kim, H.J., Sung, Y.E., Kim, W.B. (2008). Porous Cobalt Oxide Thin Films from Low Temperature Solution Phase Synthesis for Electrochromic Electrode. *Thin Solid Films*, 516: 8573-8578.

[31] Jongsomjit, B., Panpranot, J., Goodwin Jr., J.G. (2001). Co-Support Compound Formation in Alumina-Supported Cobalt Catalysts. *Journal of Catalysis*, 204: 98-109.

[32] Ataloglou, T., Vakros, J., Bourikas, K., Fountzoula, C., Kordulis, C., Lycourghiotis, A. (2005). Influence of the Preparation Method on the Structure–Activity of Cobalt Oxide Catalysts Supported on Alumina for Complete Benzene Oxidation. *Applied Catalysis B: Environmental*, 57: 299-312.

[33] Okamoto, Y., Nagata, K., Adachi, T., Imanaka, T., Inamura, K., Takyu, T. (1991). Preparation and Characterization of Highly Dispersed Cobalt Oxide and Sulfide Catalysts Supported on SiO$_2$. *The Journal of Physical Chemistry*, 95: 310-319.

[34] Sun, H., Liang, H., Zhou, G., Wang, S. (2013). Supported Cobalt Catalysts by One-Pot Aqueous Combustion Synthesis for Catalytic Phenol Degradation. *Journal of Colloid and Interface Science*, 394: 394-400.

[35] Khodakov, A.Y., Griboval-Constant, A., Bechara, R., Zholobenko, V.L. (2002). Pore Size Effects in Fischer Tropsch Synthesis over Cobalt-Supported Mesoporous Silicas. *Journal of Catalysis*, 206: 230-241.

[36] Todorova, S., Pârvulescu, V., Kadinov, G., Tenchev, K., Somacescu, S., Su, B.L. (2008). Metal States in Cobalt- and Cobalt–Vanadium-Modified MCM-41 Mesoporous Silica Catalysts and their Activity in Selective Hydrocarbons Oxidation. *Microporous and Mesoporous Materials*, 113: 22-30.

[37] Ataloglou, T., Fountzoula, C., Bourikas, K., Vakros, J., Lycourghiotis, A., Kordulis, C. (2005). Cobalt Oxide/γ-Alumina Catalysts Prepared by Equilibrium Deposition Filtration: The Influence of the Initial Cobalt Concentration on the Structure of the Oxide Phase and the Activity for Complete Benzene Oxidation. *Applied Catalysis A: General*, 288: 1-9.

[38] Yuan, Z.Y., Chen, T.H., Wang, J.Z., Li, H.X. (2001). Synthesis and Characterization of Silicon and Cobalt Substituted Mesoporous Aluminophosphates. *Colloids and Surfaces A: Physicochemical and Engineering Aspects*, 179: 253-259.

[39] Das, T., Deo, G. (2011). Synthesis, Characterization and In Situ DRIFTS during the CO$_2$ Hydrogenation Reaction over Supported Cobalt Catalysts. *Journal of Molecular Catalysis A: Chemical*, 350: 75-82.

[40] Solsona, B., Davies, T.E., Garcia, T., Vázquez, I., Dejoz, A., Taylor, S.H. (2008). Total Oxidation of Propane using Nanocrystalline Cobalt Oxide and Supported Cobalt Oxide Catalysts. *Applied Catalysis B: Environmental*, 84: 176-184.

[41] Das, T., Deo, G. (2012). Effects of Metal Loading and Support for Supported Cobalt Catalyst. *Catalysis Today*, 198: 116-124

[42] Trigueiro, F.E., Ferreira, C.M., Volta, J.C., Gonzalez, W.A., Pries de Oliveria, P.G. (2006). Effect of Niobium Addition to Co/γ-Al$_2$O$_3$ Catalyst on Methane Combustion. *Catalysis Today*, 118: 425-32.

[43] El-Korso, S., Rekkab, I., Choukchou-Braham, A., Bedrane, S., Pirault-Roy, L., Kappenstein, C. (2012). Synthesis of Vanadium Oxides 5 wt.% VO$_2$–M$_x$O$_y$ by Sol–Gel Process and Application in Cyclohexene Epoxidation. *Bulletin of Materials Science*, 35: 1187-1194.

[44] El-Korso, S., Khaldi, I., Bedrane, S., Choukchou-Braham, A., Thibault-Starzyk, F., Bachir, R. (2014). Liquid Phase Cyclohexene Oxidation over Vanadia Based Catalysts with Tert-Butyl Hydroperoxide: Epoxidation versus Allylic Oxidation. *Journal of Molecular Catalysis A: Chemical*, 394: 89-96.

[45] Ziolek, M. (2003). Niobium-Containing Catalysts-The State of the Art. *Catalysis Today*, 78: 47-64.

[46] Martínez-Méndez, S., Henríquez, Y., Domínguez, O., D'Ornelas, L., Krentzien, H. (2006). Catalytic Properties of Silica Supported Titanium, Vanadium and Niobium Oxide Nanoparticles towards the Oxidation of Saturated and Unsaturated Hydrocarbons. *Journal of Molecular Catalysis A: Chemical*, 252: 226-234.

[47] Rothenberg, G., Wiener, H., Sasson, Y. (1998). Pyridines as Bifunctional Co-Catalysts in the CrO$_3$-Catalyzed Oxygenation

of Olefins by T-Butyl Hydroperoxide. *Journal of Molecular Catalysis A: Chemical*, 136: 253-262.

[48] Bonneviot, L., Beland, F., Danumah, C., Giasson, S., Kaliaguine, S. (1998). *Mesoporous Molecular Sieves*, Press

[49] Salavati-Niasari, M., Elzami, M.R., Mansournia, M.R., Hydarzadeh, S. (2004). Alumina-Supported Vanadyl Complexes as Catalysts for the CH Bond Activation of Cyclohexene with Tert-Butylhydroperoxide. *Journal of Molecular Catalysis A: Chemical*, 221: 169-175.

[50] Ganji, S., Bukya, P., Vakati, V., Raoa, K.S.R., Burri, D.R. (2013). Highly Efficient and Expeditious PdO/SBA-15 Catalysts for Allylic Oxidation of Cyclohexene to Cyclohexenone. *Catalysis Science & Technology*, 3: 409-414.

[51] Ghiaci, M., Aghabarari, B., Botelho do Rego, A.M., Ferraria, A.M., Habibollahi, S. (2011). Efficient Allylic Oxidation of Cyclohexene Catalyzed by Trimetallic Hybrid Nano-Mixed Oxide (Ru/Co/Ce). *Applied Catalysis A: General*, 393: 225-230.